Electronic Supplementary Information

Accelerating Reaction Modeling Using Dynamic Flow Experiments, Part 1: Design Space Exploration

Peter Sagmeister,[a,b] Christine Schiller,[a,b] Peter Weiss, [a] Klara Silber,[a,b] Sebastian Knoll,[c] Martin Horn,[c] Christopher A. Hone,[a,b] Jason D. Williams*[a,b] and C. Oliver Kappe*[a,b]

[a]Center for Continuous Flow Synthesis and Processing (CC FLOW), Research Center Pharmaceutical Engineering GmbH (RCPE), Inffeldgasse 13, Graz, Austria

[b]Institute of Chemistry, University of Graz, Heinrichstrasse 28, 8010 Graz, Austria.

[c]Institute of Automation and Control, Graz University of Technology, Inffeldgasse 21b, 8010 Graz, Austria

Email: jason.williams@rcpe.at, oliver.kappe@uni-graz.at

Table of Contents

1   General Information

1.1   Materials and Flow Equipment

Solvents and chemicals were obtained from commercial suppliers and were used without any further purification unless otherwise noted. In the flow setup, standard PFA tubing (0.8 mm or 1.6 mm i.d.), fittings, T-pieces manufactured from PTFE or PEEK were used as connectors. The back pressure regulator was obtained from Upchurch Scientific.

2   General Flow Configuration

Input solutions were prepared with the following procedure.

5.0 M 1,2,4-triazole (**1**) stock solution: In a 250 mL volumetric flask 86.4 g of **1** and 14.5 g of biphenyl were dissolved in MeOH and filled up to the 250 mL mark with MeOH.

0.5 M DIPEA (**2**) stock solution: In a 250 mL volumetric flask 16.15 g of **2** was dissolved in MeOH and filled up to the 250 mL mark with MeOH.

7.5 M acrylonitrile (**3**) stock solution: In a 200 mL volumetric flask 79.6 g of **3** was dissolved in MeOH and filled up to the 200 mL mark with MeOH.

The MeOH feed was prepared in quantities of 500 mL.

The reaction was performed in a Modular MicroReaction System (MMRS) from Ehrfeld Mikrotechnik, the reaction stream was analyzed by a ReactIR 15 instrument from Mettler Toledo and a 43 MHz Spinsolve Ultra benchtop NMR from Magritek (**Figure S1**).
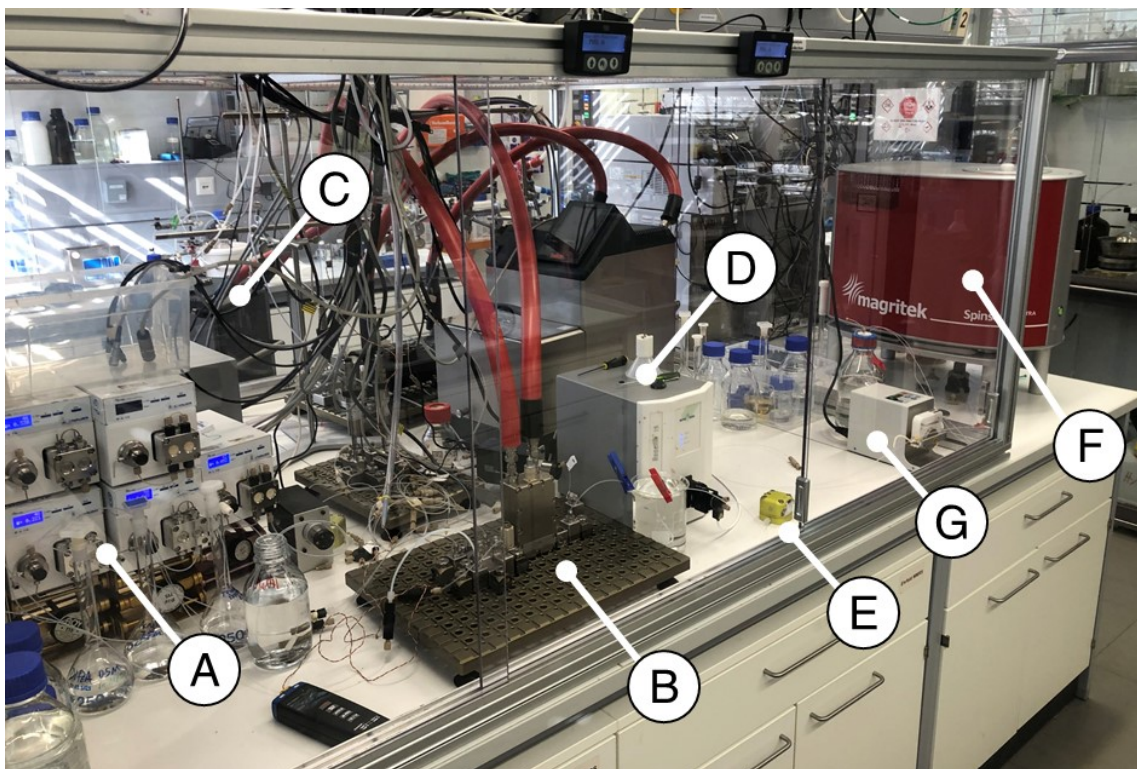
Figure S1. Photograph of reaction setup in the lab, showing the following equipment: A: HPLC Pumps, B: MMRS, C: Thermostat, D: inline FTIR, E: BPR, F: online NMR, G: peristaltic pump

All four feeds solutions were pumped with Knauer AZURA P 4.1S HPLC pumps (10 mL/min pump head, made of Hastelloy C/stainless steel/ceramic with an integrated pressure sensor). A back pressure regulator (BPRs, Upchurch cartridge holder, P-465) equipped with a 34 bar (tan/green, P-765) cartridge was connected directly after each HPLC pump, prior to entering the MMRS system. The arrangement of the different modules on the MMRS system is shown in **Figure S2**.

The feed containing **1** entered the MMRS system through a 1/16" input connector (0711-2-0124-F, Hastelloy C-276), followed by a pressure sensor module (0518-1-60x4-F, Hastelloy C-276), and was mixed in a T-type connecting module (0723-1-0004, Hastelloy C-276) with the feed containing **3**, which entered through a 1/16" input connector (0711-2-0124-F, Hastelloy C-276). The feed containing MeOH entered the MMRS system through a 1/16" input connector (0711-2-0124-F, Hastelloy C-276), followed by a pressure sensor module (0518-1-60x4-F, Hastelloy C-276), and was mixed in a T-type connecting module (0723-1-0004, Hastelloy C-276) with the feed containing **2**, which entered through a 1/16" input connectors (0711-2-0124-F, Hastelloy C-276). The stream containing **1** and **3** was mixed with the stream containing MeOH and **2** in a cascade mixer 06 (0216-3-0014-F, mixing structure 10 µL, Hastelloy C-276), followed by a temperature sensor module (0501-2-1004-X, Hastelloy C-276). The next module on the MMRS was a capillary reactor (0214-1-1004-F, built in connection body of 2.04 mL, Hastelloy C-276), whose temperature was controlled by a thermostat (Huber, Ministat 240). After the capillary reactor, the reaction solution passed through a temperature dividing module (0724-3-0004, Hastelloy C-276) and exited the MMRS system via a 1/16" in/out connector (0711-2-0124-F, Hastelloy C-276).

The reaction mixture was cooled after the MMRS to room temperature in an additional PFA tube (0.31 mL, 0.8 mm i.d.), which was placed in a water bath. The end of the PFA tubing was connected to the flow cell (Mettler Toledo, Micro Flow Cell DS SiComp) of the FTIR (Mettler Toledo, ReactIR 15) and analyzed. The outlet of the flow cell was connected with a PFA tube (0.1 mL, 0.8 mm i.d.) to a membrane-based BPR (Zaiput, BPR-10), which was set to 15 bar. The outlet of the BPR was connected to a T-piece with a PFA tubing (0.6 mL, 0.8 mm i.d.).

The reaction stream was subsampled at this point: a fraction of the reaction stream was diverted with a PFA tube (0.15 mL, 0.8 mm i.d.) to a 6-port valve (0.05 mL). This 6-port valve was installed prior to the glass flow cell (800 µL internal volume, 550 mm length), allowing the NMR to be bypassed in case the instrument needed to be re-shimmed (Figure S3). The reaction stream left the NMR through PFA tubing (0.3 mL, 0.8 mm i.d.) and a peristaltic pump (Ismatec, ISM834C set to a flow rate of 0.5 mL/min), which was pumping the reaction solution out of the subsampling point. Both streams from the NMR and the subsampling point were collected in the receiver vessel.

Note: for the steady-state experiments, the peristaltic pump was placed between the 6-port valve and the subsampling point, but this was later moved downstream of the NMR to minimize volume prior to analysis (see **Figure S9** vs **Figure S10**).
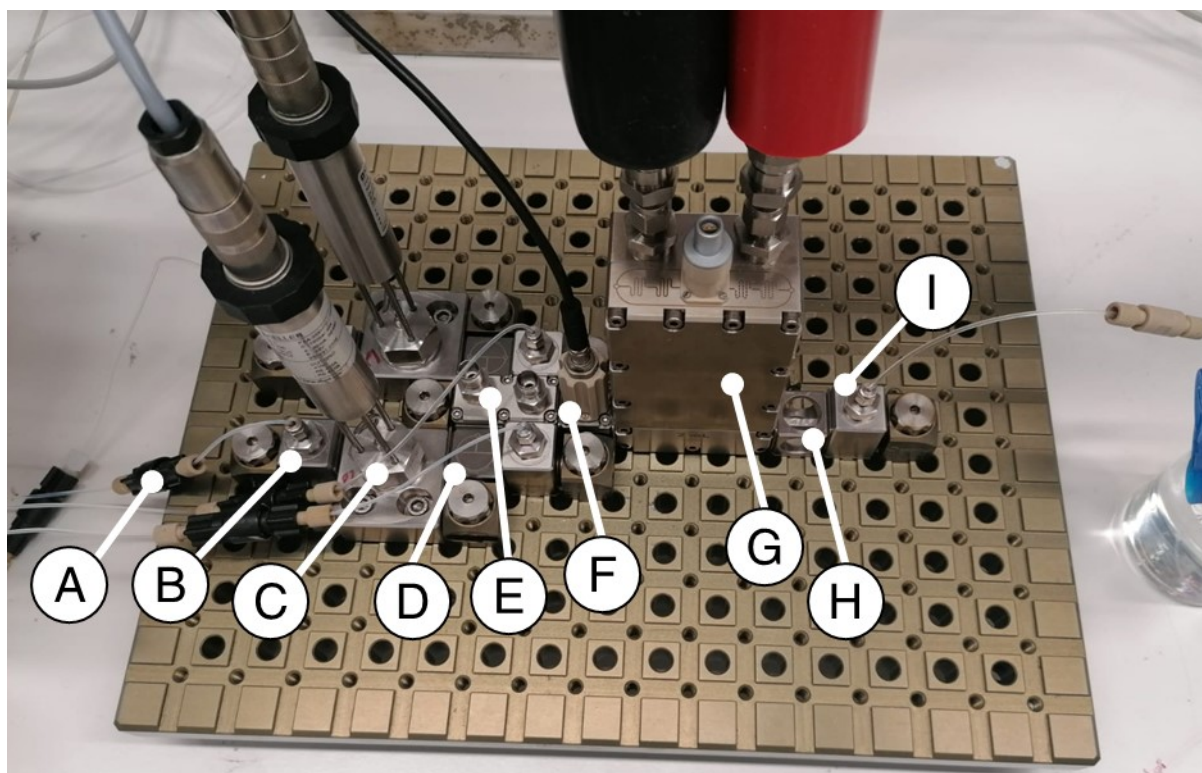
Figure S2. Photograph of the arrangement of the parts on the MMRS system. A: Upchurch BPR, B: Inlet module, C: pressure sensor, D: T-type connecting module, E: Cascade mixer, F: temperature sensor, G: capillary reactor, H: temperature dividing module, I: outlet module.
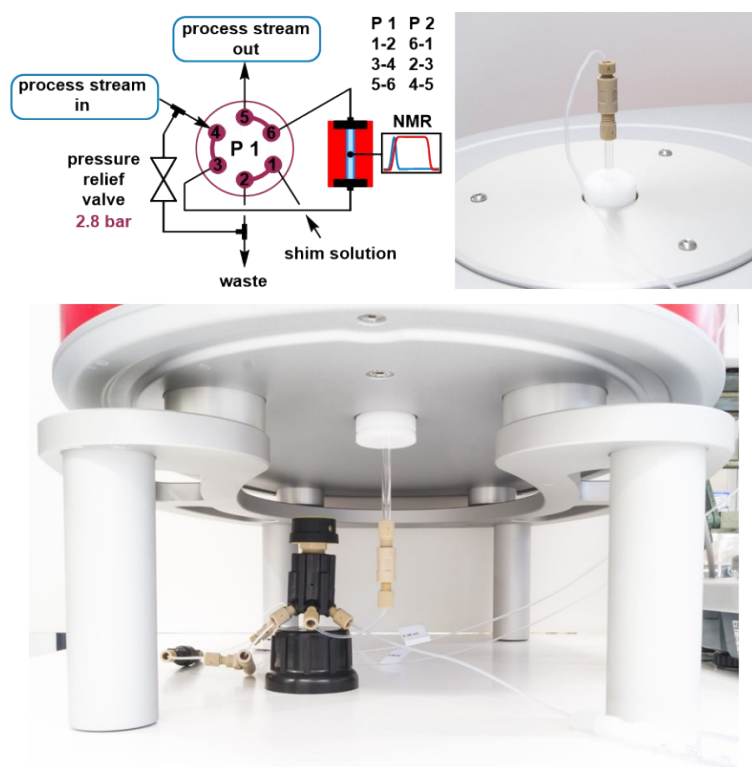
Figure S3. An overview of the NMR configuration using the glass flow cell and 6-port valve, which can be used to divert the flow around the NMR if necessary.

3 Automation

The HPLC pumps and the thermostat were connected via RS232 to the LabManager (HiTec Zang). The ramps for the flow rates and temperature were programmed in HiText (HiTec Zang) and the setpoints for the HPLC pumps and the thermostat were set in the LabVision software (HiTec Zang).

3.1 HiText Script

The pump flow rates were controlled throughout the experiments by the following scripts. Each variable was changed over time (as described in **Table S2**), and the flow rates were adapted automatically.

3.1.1 Script for Pump 1

```
variable
c_sub:Float = 5.0 {mol/L} {stock solution triazole}
c_reag:Float = 7.5 {mol/L} {stock solution acrylonitrile}
flowrate_tot:Float
flowrate_init_sub:Float
VARIABLE_1:Float          {equivalents of acrylonitrile}
VARIABLE_2:Float          {residence time in minutes}
VARIABLE_3:Float          {1, 2, 4, triazole concentration}
end variable

begin
    flowrate_tot = 2/(!VARIABLE_2/60)
    flowrate_init_sub    =    (flowrate_tot    *    !VARIABLE_1    *
    (c_sub/c_reag))/(1+(!VARIABLE_1* (c_sub/c_reag)))
    !HPLC_PUMP_1.F_W    =    flowrate_init_sub/(((flowrate_init_sub*c_sub)
    /flowrate_tot) /!VARIABLE_3)

goto begin
```

3.1.2 Script for Pump 2

```
variable
c_sub:Float = 5.0 {mol/L} {stock solution triazole}
c_reag:Float = 7.5 {mol/L} {stock solution acrylonitrile}
VARIABLE_1:Float          {equivalents of acrylonitrile}    end variable

begin
    !HPLC_PUMP_2.F_W = (!HPLC_PUMP_1.F_W * !VARIABLE_1 *c_sub ) / c_reag
goto begin
```

3.1.3 Script for Pump 3

```
variable
flowrate_tot:Float
VARIABLE_2:Float          {residence time in minutes}
end variable

begin
    flowrate_tot = 2/(!VARIABLE_2/60)
    !HPLC_PUMP_3.F_W = flowrate_tot - !HPLC_PUMP_1.F_W - !HPLC_PUMP_2.F_W -
    !HPLC_PUMP_4.F_W
```

```
goto begin
```

3.1.4   Script for Pump 4

```
variable
c_sub:Float = 5.0 {mol/L} {stock solution triazole}
c_base:Float = 0.5 {mol/L} {stock solution DIPEA}
VARIABLE_4:Float            {equivalents of DIPEA)
end variable
```
```
begin
      !HPLC_PUMP_5.F_W = (!HPLC_PUMP_1.F_W * !VARIABLE_4 *c_sub) / c_base
goto begin
```

4   Process Analytical Technology (PAT)

4.1   Inline FTIR

Inline FT-IR spectra were recorded on a ReactIR 15 instrument (Mettler Toledo, ReactIR 15) equipped with a flow through cell (Mettler Toledo, Micro Flow Cell DS SiComp). The acquisition time for each data point was 15 s and spectra were recorded between 4000 and 600 cm^{-1} using the maximum resolution of 4 cm^{-1}. It was ensured that the MCT detector was initially warmed up, then cooled with liquid N_2, the peak height between 18000 and 24000 and the signal to noise ratio was above 5000. The obtained spectra were exported by the iCIR7 software and automatically read and processed with a PLS model by ProcessLink (S-PACT).

4.1.1   PLS Model

The training samples were obtained from steady-state operation points. In total, 16 different levels, each including 10 to 20 spectra, were used to develop the PLS model in PEAXACT 5.3 software (S-PACT). The acquired training set was read into PEAXACT and processed with the same pretreatment conditions. The global range was set to 3060 to 650 cm^{-1} and a rubber band subtraction was used for a baseline correction. The reduced spectra were further processed using the 1st order derivative with a filter length of 5. An example spectrum is shown in **Figure S4**, before and after pre-processing was applied.

In the calibration model the following ranks were set for each component: 1,2,4-triazole **1** (rank 8), product **4** (rank 5) and side product **5** (rank 7). The calibration model provided a performance indicator of model error: the root-mean-square error of calibration ($RMSE_C$). Additionally, to perform cross-validation and evaluate the root-mean-square error of cross validation ($RMSE_{CV}$), the training set was divided in subgroups, based on their concentration levels. The predicted vs. true plots for the finalized models, including the ranks, $RMSE_C$ and $RMSE_{CV}$ are shown in **Figure S5**.
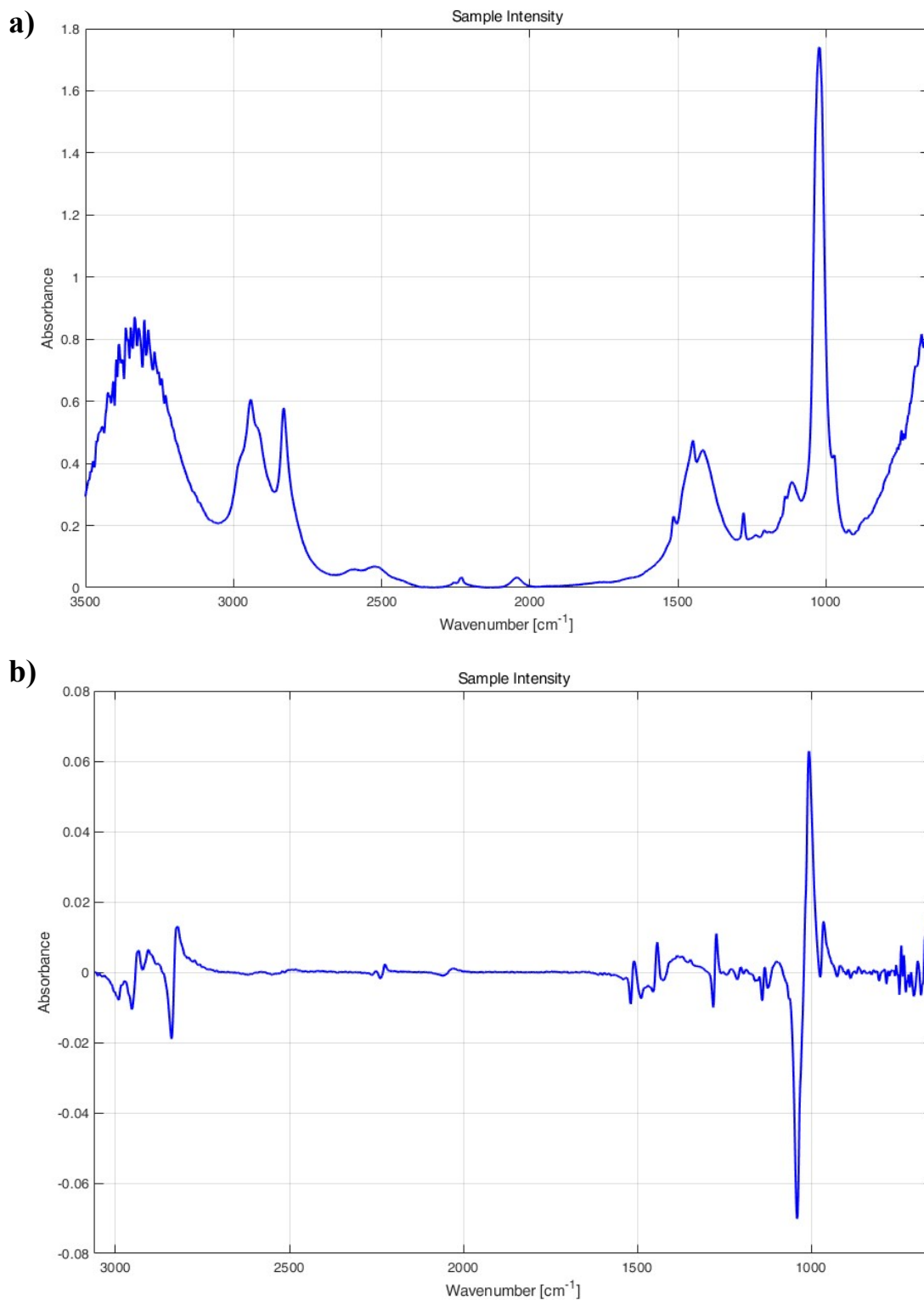
Figure S4. Example IR spectrum from PLS calibration set ([triazole **1**] = 0.328 M, [product **4**] = 0.289 M, [regioisomer **5**] = 0.068 M). a) Spectrum prior to pre-processing. b) Spectrum after pre-processing, as detailed above.
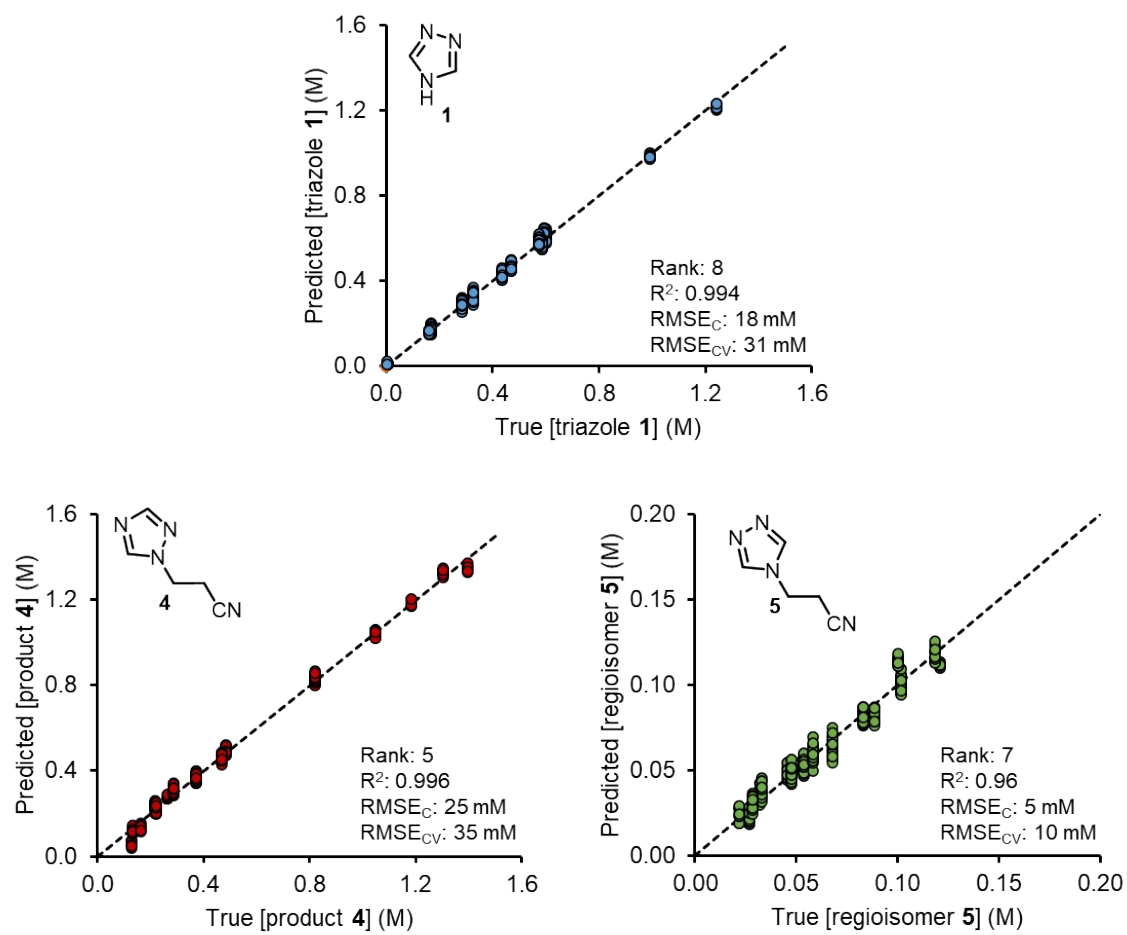
Figure S5. Predicted vs. true plots of the triazole **1** (top) and the products **4** and **5** (bottom).

4.2 Online NMR

Online NMR reaction monitoring was accomplished by recording ^{1}H spectra using a low field benchtop 43.795 MHz NMR spectrometer (Magritek, Spinsolve Ultra 43 MHz). Shims were performed with the flow cell filled with either reaction mixture or a MeOH solution and referenced to the MeOH peak at 3.34 ppm. Typically, a "QUICKSHIM: ALL" was performed in the Spinsolve software (Magritek) and shim values were below 0.4 Hz linewidth at 50%, below 7.5 Hz linewidth at 0.55% and a signal to noise ratio above 20,000.

The spectra were typically recorded in the reaction monitoring mode with a pulse angle of 90 °, acquisition time of 6.4 s, repetition time of 10.0 s and a single scan. The recorded spectra were automatically read and processed with an indirect hard model by ProcessLink (S-PACT).

4.2.1 Indirect Hard Model

The indirect hard model was developed in PEAXACT 5.3 software (S-PACT). The pretreatment model was used on each acquired NMR spectrum. The pretreatment included apodization (exponential with 0.2 Hz), zero filling (65536) and a phase correction (auto, negative peak penalization). Each spectrum was aligned against the MeOH signal at the target position of 3.34. Additionally, the range of 2.068 ppm to 5.158 ppm was excluded and a straight line subtraction was used for baseline correction. An indirect hard model was fitted for the triazole **1**, DIPEA **2**, acrylonitrile **3**, product **4**, and regioisomer **5** and calibrated with a one-point calibration. The individual indirect hard models for the triazole **1**, product **4** and regioisomer **5** are shown in **Figure S6**.
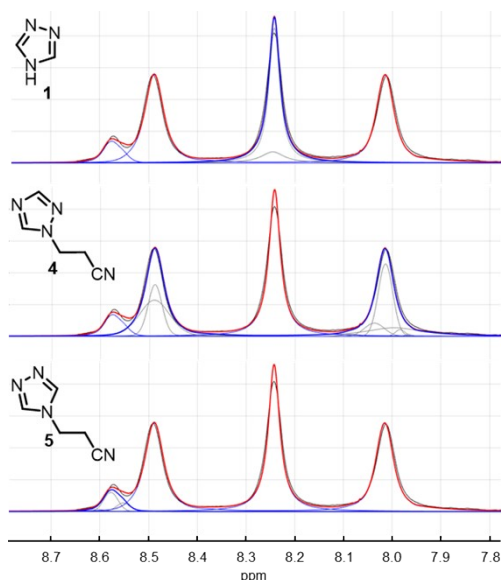
Figure S6. The indirect hard models for the triazole **1**, product **4** and regioisomer **5**. The acquired spectrum is in black. The individual hard model of each compound is in blue and the mixture model in red.

5 Residence Time Distribution
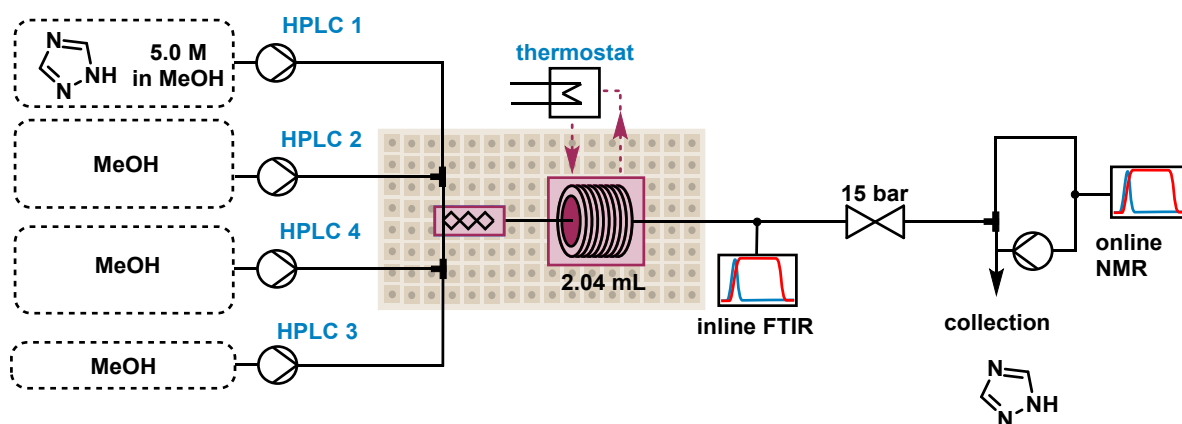
Figure S7. Detailed flow setup for the residence time distribution experiments.

The process setup is described in section 2 with minor modifications for the feed solutions. The pump used to subsample out of the process stream for the NMR was placed after the NMR. See **Figure S7** for the configuration. The residence time distribution was automatically screened at three different temperatures (25 °C, 100 °C and 140 °C) and at three different residence times (180 s, 90 s, and 30 s). Each residence time was investigated in duplicates by changing the concentration of triazole **1** by a step up (0 M to 1 M) and a step down (1 M to 0 M). The change of process parameters for the residence time distribution experiment are displayed in **Figure S8**. Detailed discussion of the RTD results (including calculated measures of dispersion) can be found in part 2 of the publication.
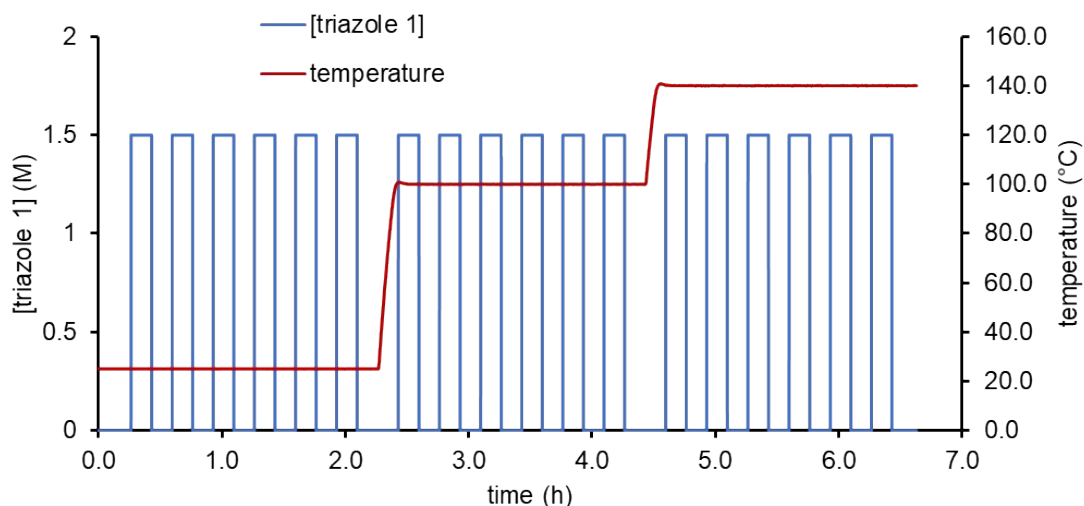
Figure S8. Change of concentration of triazole **1** and the temperature during the residence time distribution experiments.

6   Steady State Experiments

Figure S9. Detailed flow setup for the steady state experiments.

The process setup is described in section 2. The pump used to subsample out of the process stream for the NMR was placed before the NMR. See **Figure S9** for the configuration. A summary of the steady-state results is provided in **Table S1**.
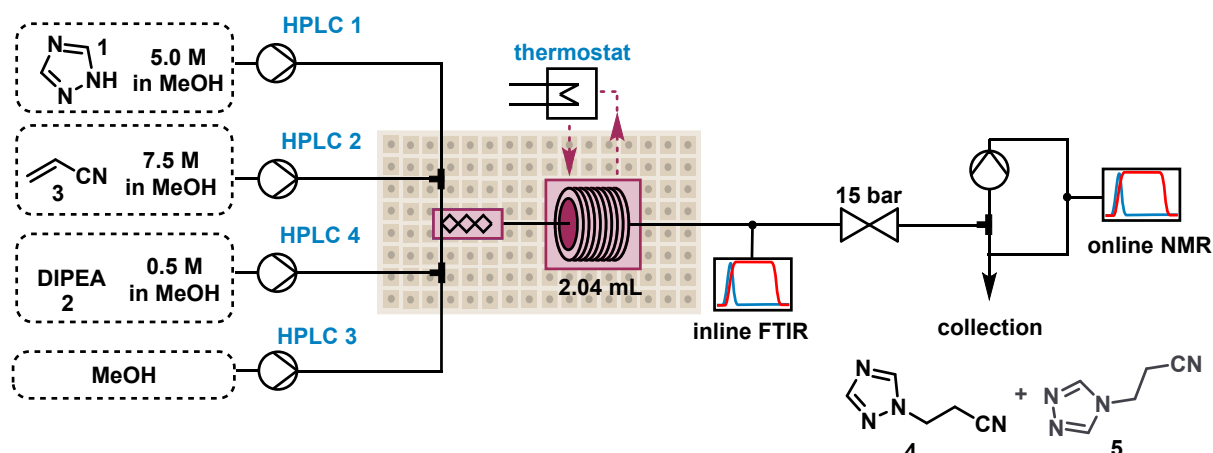
Table S1. Summary of the process conditions and results for the steady state experiments.

| Entry | Ratio 3/1 | [1] | RT | Temp | Ratio 2/1 | Measured at NMR | | | |
| | | | | | | [1] | [3] | [4] | [5] |
		(mol/L)	(s)	(°C)		(M)	(M)	(M)	(M)
1	2.0	1.50	30	100	0.10	1.242	2.577	0.265	0.022
2	2.0	1.50	60	100	0.10	0.992	2.278	0.483	0.045
3	2.0	1.50	120	100	0.10	0.601	1.900	0.820	0.083
4	2.0	1.50	180	100	0.10	0.326	1.638	1.046	0.102
5	1.5	0.75	30	120	0.10	0.672	0.984	0.205	0.025
6	1.5	0.75	60	120	0.10	0.585	0.877	0.132	0.033
7	1.5	0.75	120	120	0.10	0.436	0.742	0.219	0.054
8	1.5	0.75	180	120	0.10	0.328	0.676	0.289	0.068
9	2.0	0.75	30	140	0.05	0.575	1.098	0.164	0.027
10	2.0	0.75	60	140	0.05	0.469	1.114	0.223	0.028
11	2.0	0.75	120	140	0.05	0.285	1.199	0.372	0.048
12	2.0	0.75	180	140	0.05	0.170	1.063	0.469	0.058
13	2.0	1.50	30	140	0.10	0.572	1.847	0.821	0.089
14	2.0	1.50	60	140	0.10	0.161	1.493	1.183	0.121
15	2.0	1.50	120	140	0.10	0.005	1.448	1.305	0.118
16	2.0	1.50	180	140	0.10	0.005	1.381	1.394	0.101

7 Dynamic Experiments
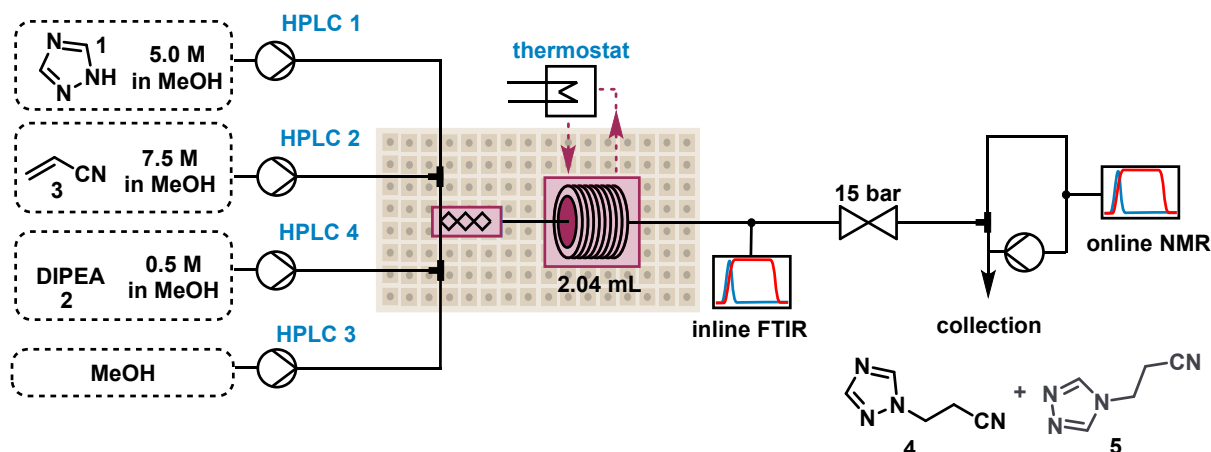
Figure S10. Detailed flow setup for the dynamic experiments.

The process setup is described in section 2. The pump used to subsample out of the process stream for the NMR was placed after the NMR. See **Figure S10** for the configuration. A summary of the varied process conditions (beginning and end point) is provided in **Table S2**. The recorded data for the dynamic runs is published as open access dataset on Zenodo.[1]

Table S2. Summary of process conditions for the dynamic experiments.

Experiment	Run	Residence time (s)	Temperature (°C)	[1] (M)	equiv acrylonitrile 3	equiv DIPEA 2
2	1	60	100-140-100	1.5	2.0	0.1
2	2	52	100-140-100	0.65	2.0	0.2
2	3	60	100-140-100	1.0	1.1	0.075
3	1	120	120	1.5	2.0-0.8	0.1
3	2	80	120	0.75-1.5	1.5	0.1
3	3	70	140	1.5	2.0	0-0.1
3	4	120	140-100-140-100	1.5	2.0-0.8-2.0	0.1
3	5	80	140-100-140-100	0.75-1.5-0.75	2.0-0.8-2.0	0.1
4	1	180-30-180-30	120	1.5	2.0-0.8-2.0	0.1
5	1	180-30-180-30	120-140-100-120	1.5	2.0-0.8-2.0	0.1
6	1	180-30-180-30	120-140-100-120	0.75-1.5-0.75-1.5-0.75	2.0-0.8-2.0	0.1
7	1	180-30-180-30	120-140-100-120	0.75-1.5-0.75-1.5-0.75	2.0-0.8-2.0	0.1-0.01-0.1-0.01

8 Development of Fitting Program in Matlab

Kinetic parameter fitting and concentration predictions were performed using a custom Matlab script, written on Matlab R2022b (9.13.0). The only nonstandard toolbox required is the "Control System Toolbox". The workflow is described roughly in the flowchart below (**Figure S11**), including a side loop, only used to fit the kinetic parameters.
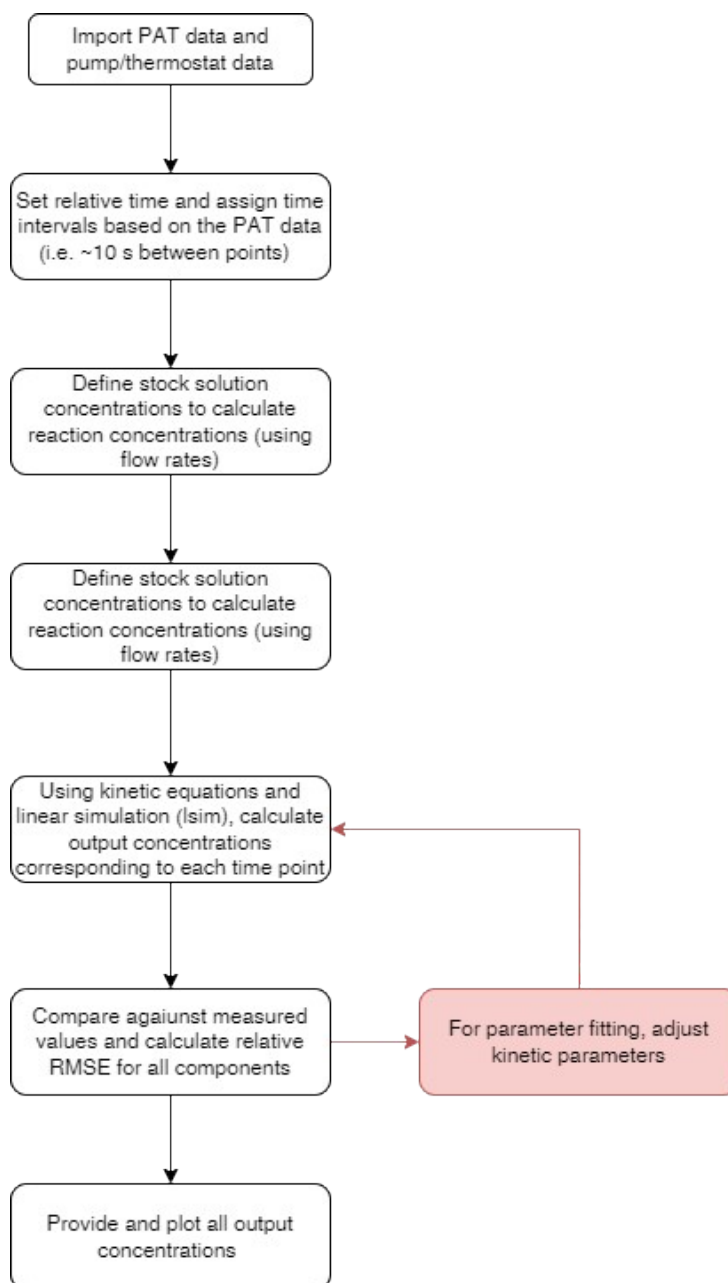
Figure S11. Flow chart showing the workflow followed by the Matlab program. The boxes in red are only followed for parameter fitting experiments, where this loop is iterated through numerous times (200 × number of parameters to be fitted = 2000 iterations) to minimize the error between predicted and measured concentrations.

9   Kinetic Parameters

The following kinetic equation was parameterized for each of the three different experiment types. The reaction scheme is shown below, with equations 1 and 2. The optimized kinetic parameters are summarized in **Table S3**.
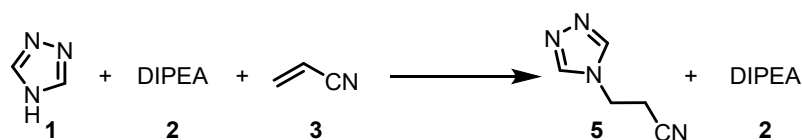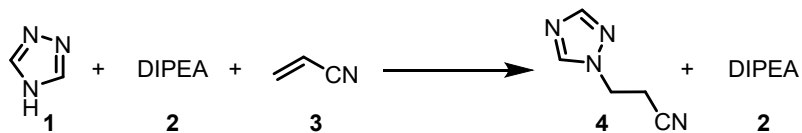
$$\frac{d[4]}{dt} = A_1 e^{\frac{-Ea1}{RT}} [1]^{a1}[2]^{b1}[3]^{c1} \tag{1}$$

$$\frac{d[5]}{dt} = A_2 e^{\frac{-Ea2}{RT}} [1]^{a2}[2]^{b2}[3]^{c2} \tag{2}$$

Table S3. Summary of kinetic parameters for each of the three models discussed in the manuscript.

Parameter	Steady State	Dynamic	Multi-ramp
A_1	493.8	940.8134	311.8970
Ea1 (J/mol)	35100	38051	32179
a1	0.64	0.3232	0.3883
b1	1.47	1.5418	1.3089
c1	0.5	0.4893	0.6127
A_2	317.0	434.9603	379.2799
Ea2 (J/mol)	38400	37696	39233
a2	1.12	0.6493	0.2206
b2	0.5	0.3483	0.6080
c2	0.5	0.7452	0.5940

10   Additional Dynamic Experiment Data

Graphs showing the predicted and measured results for each of the described experiments are shown below. The predictions were made using the final "multi-ramp" model.

10.1   Experiment 1
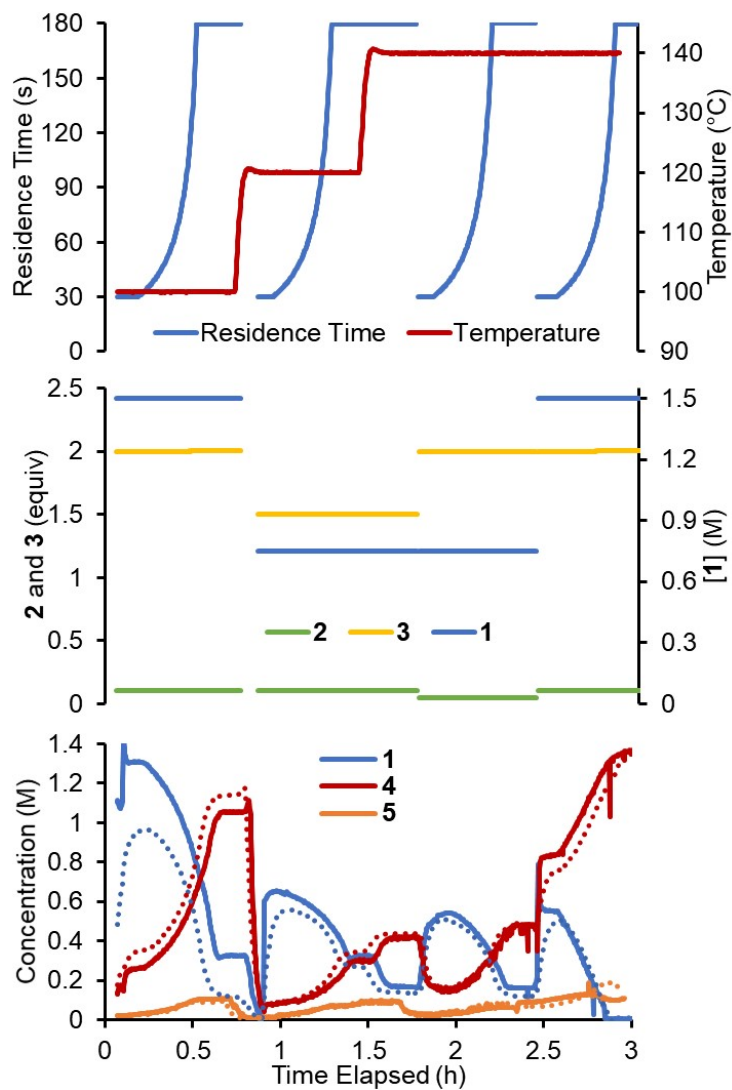
Figure S12. Data for experiment 1 in flow. Top: Residence time and temperature as varied over the experiment duration. Middle: Concentration of 1 and equivalents of 2 and 3 over the experiment duration. Bottom: Concentrations of reaction species measured over the experiment duration (solid lines) and their corresponding predicted values using the multi-ramp model (dotted lines).

10.2 Experiment 2
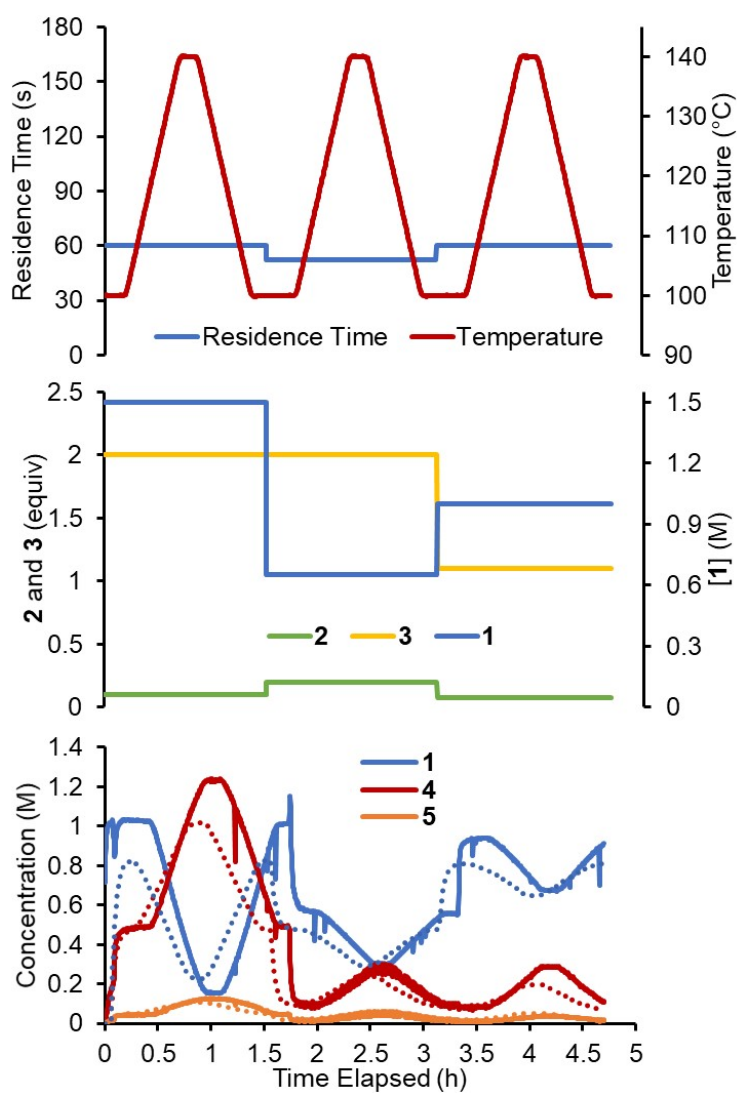
Figure S13. Data for experiment 2 in flow. Top: Residence time and temperature as varied over the experiment duration. Middle: Concentration of 1 and equivalents of 2 and 3 over the experiment duration. Bottom: Concentrations of reaction species measured over the experiment duration (solid lines) and their corresponding predicted values using the multi-ramp model (dotted lines).

10.3 Experiment 3

Figure S14. Data for experiment 3 in flow. Top: Residence time and temperature as varied over the experiment duration. Middle: Concentration of 1 and equivalents of 2 and 3 over the experiment duration. Bottom: Concentrations of reaction species measured over the experiment duration (solid lines) and their corresponding predicted values using the multi-ramp model (dotted lines).

10.4   Experiment 4

Figure S15. Data for experiment 4 in flow. Top: Residence time and temperature as varied over the experiment duration. Middle: Concentration of 1 and equivalents of 2 and 3 over the experiment duration. Bottom: Concentrations of reaction species measured over the experiment duration (solid lines) and their corresponding predicted values using the multi-ramp model (dotted lines).
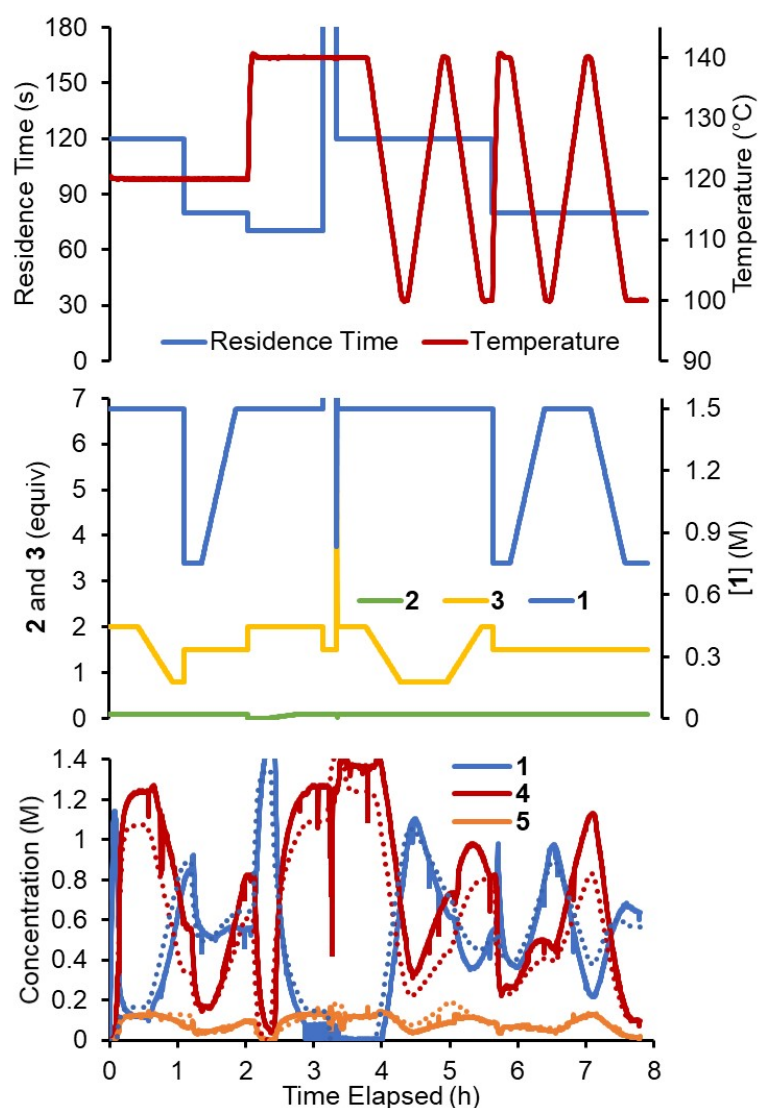
10.5 Experiment 5
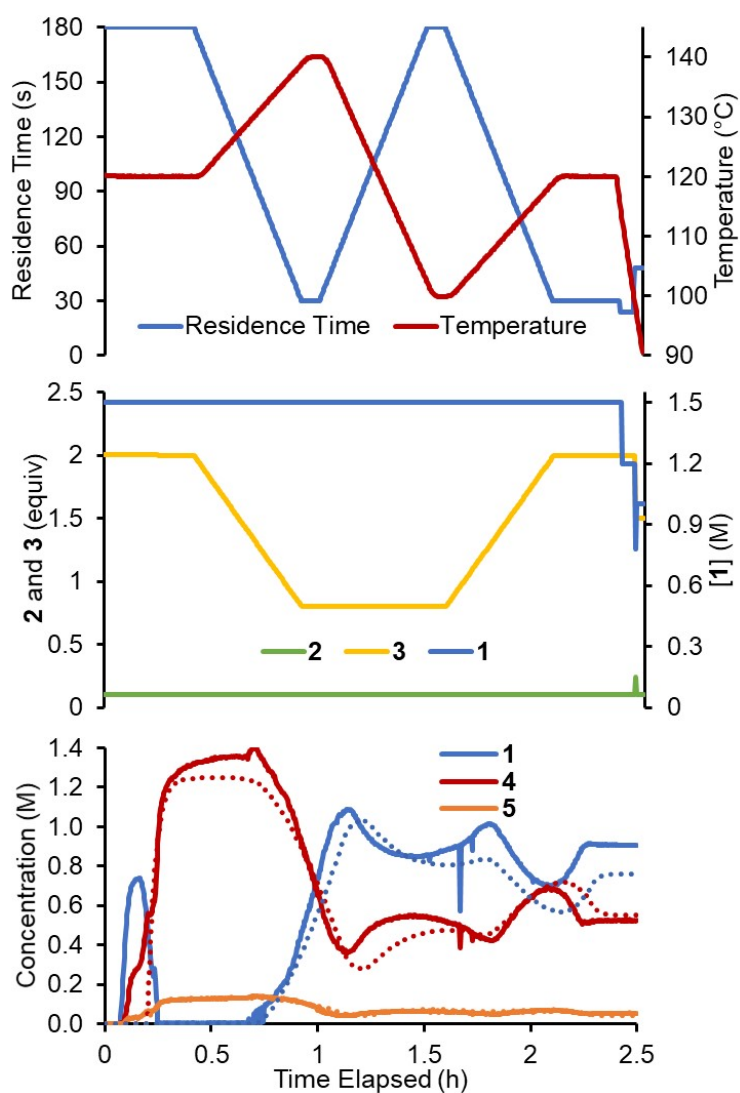
Figure S16. Data for experiment 5 in flow. Top: Residence time and temperature as varied over the experiment duration. Middle: Concentration of 1 and equivalents of 2 and 3 over the experiment duration. Bottom: Concentrations of reaction species measured over the experiment duration (solid lines) and their corresponding predicted values using the multi-ramp model (dotted lines).
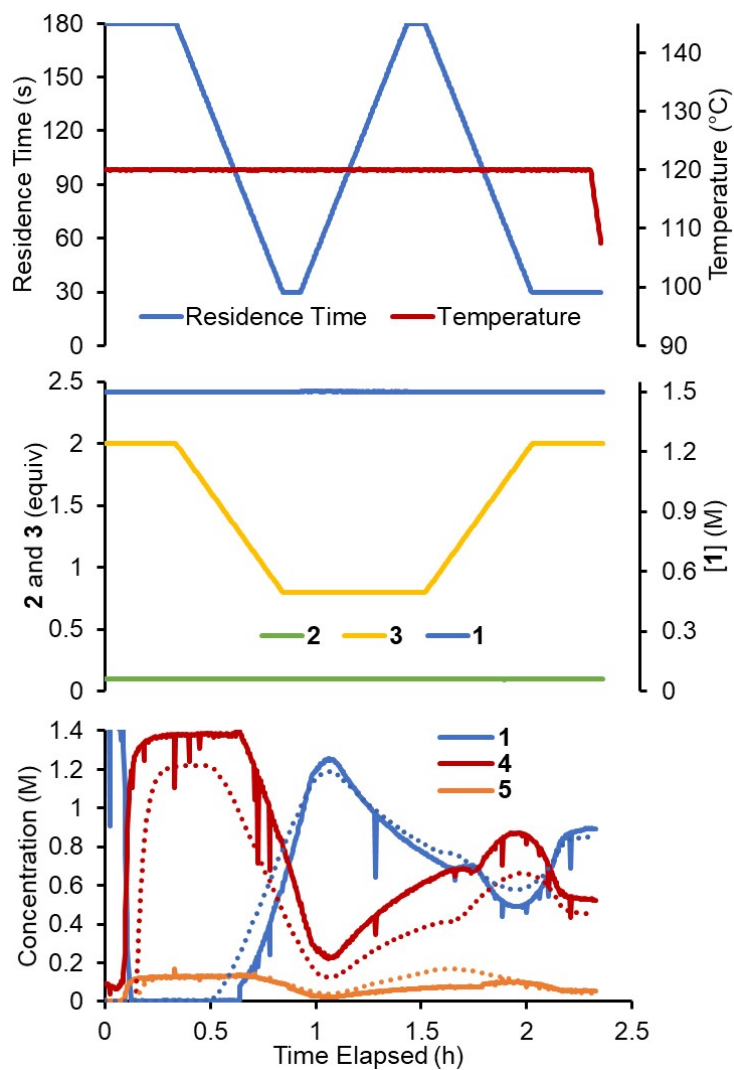
10.6   Experiment 6

Figure S17. Data for experiment 6 in flow. Top: Residence time and temperature as varied over the experiment duration. Middle: Concentration of 1 and equivalents of 2 and 3 over the experiment duration. Bottom: Concentrations of reaction species measured over the experiment duration (solid lines) and their corresponding predicted values using the multi-ramp model (dotted lines).
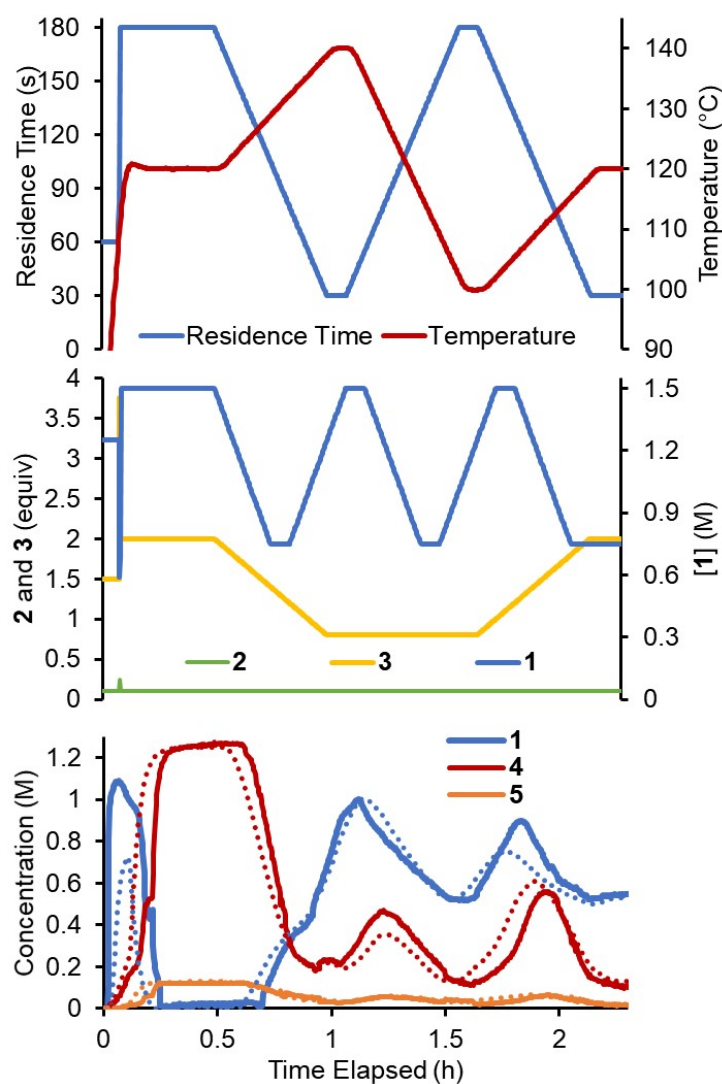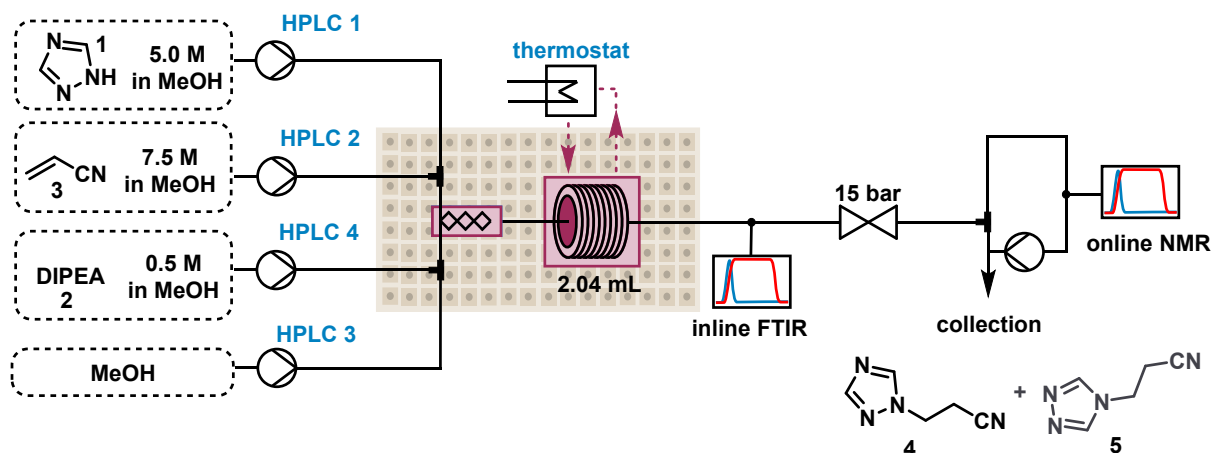
Data from experiment 7 is shown in the manuscript (Fig. 7).

11   Validation Experiments

Figure S18. Detailed flow setup for the validation experiments.

The process setup is described in section 2. The pump used to subsample out of the process stream for the NMR was placed after the NMR. See **Figure S18** for the configuration. The self-optimization platform is described in a previous publication.[2] The Thompson Sampling Efficient Multiobjective Optimization (TSEMO) algorithm[3] was used with some adaptions for the self-optimization. In the self-optimization experiments the optimization algorithm could adjust in total five different variables: ratio of acrylonitrile **3** to triazole **1**, concentration of triazole **1**, residence time, temperature of the reactor, and ratio of DIPEA **2** to triazole **1**. The upper and lower bounds of the adjustable variables can be found in **Table S4**. The objective of the optimization was to simultaneously maximize the space-time yield, conversion and minimize E-factor, as defined by **Equation 3**. The algorithm was initialized with 10 different Latin hypercube (LHC) experiments. The process conditions, the results for the self-optimization experiments can be found in **Table S5**. The comparison between predicted and measured concentrations can be found in **Table S6**.

Table S4. Lower and upper bounds of the adjustable variables in the self-optimization experiment.

Limits	Ratio **3/1**	[1] (M)	Residence time (min)	Temperature °C	Ratio **2/1**
Upper	1.0	0.6	1.0	100	0.075
Lower	2.0	1.5	3.0	140	0.200

$$minimize[-\ln(STY),\ -\ln(Conversion), \ln(E-factor)] \qquad (3)$$

Table S5. The different process conditions used in the different self-optimization experiments. The comparison of the experimental collected data points to the kinetic model.

Entry	Variables					Objectives		
	Ratio **3/1**	**[1]** (mol/L)	Res time (min)	Temp (°C)	Ratio **2/1**	STY (kg/L/h)	Conversion (%)	E-factor
1 (LHC)	1.551	1.31	2.77	103.27	0.0837	1.57	46%	9.89
2 (LHC)	1.889	1.04	2.31	107.68	0.1276	1.75	56%	10.72
3 (LHC)	1.151	0.86	2.59	109.25	0.1569	0.74	36%	23.85
4 (LHC)	1.310	0.94	1.04	113.02	0.1439	1.44	21%	30.88
5 (LHC)	1.406	1.37	2.20	119.24	0.1696	3.14	81%	5.88
6 (LHC)	1.058	1.07	1.55	121.81	0.1884	2.01	41%	14.18
7 (LHC)	1.763	0.64	1.67	124.88	0.1023	0.80	29%	34.44
8 (LHC)	1.610	1.4	1.85	129.5	0.0936	4.16	82%	5.14
9 (LHC)	1.266	1.1	1.27	134.53	0.1186	3.26	53%	10.45
10 (LHC)	1.995	0.7	2.93	138.81	0.1778	1.59	100%	9.21
11	1.202	1.40	2.18	140.0	0.1872	3.51	89%	5.20
12	1.915	1.42	2.14	136.7	0.1949	3.65	100%	5.09
13	1.942	1.49	2.99	130.8	0.1774	2.79	100%	4.69
14	1.818	1.50	2.29	139.2	0.1285	4.33	100%	3.78
15	1.964	1.48	1.86	138.9	0.1141	5.36	100%	3.76
16	2.000	1.48	1.77	138.2	0.1380	5.12	100%	4.22
17	1.523	1.39	2.50	139.0	0.1260	3.74	100%	4.06
18	1.673	1.48	2.33	138.2	0.0994	4.32	100%	3.71
19	1.692	1.46	1.97	139.7	0.1027	4.99	100%	3.83
20	1.968	1.45	1.25	139.8	0.0857	7.11	90%	4.34
21	1.793	1.42	1.36	137.7	0.0750	5.81	81%	5.01
22	2.000	1.46	2.40	140.0	0.0893	4.25	100%	3.65
23	1.532	1.47	1.81	140.0	0.1590	4.69	100%	4.58
24	1.987	1.49	2.03	138.3	0.0750	5.07	100%	3.61
25	1.925	1.50	1.61	137.1	0.0961	6.09	100%	3.84
26	1.866	1.49	1.17	138.2	0.0830	7.37	82%	4.51
27	1.853	1.45	2.16	136.0	0.0971	4.59	100%	3.78
28	1.817	1.50	2.91	140.0	0.0809	3.65	100%	3.46
29	1.831	1.38	1.65	139.7	0.0949	5.36	94%	4.37
30	1.874	1.49	1.55	138.6	0.1068	6.25	100%	3.88
31	1.959	1.46	1.53	140.0	0.1182	6.11	100%	4.06
32	1.997	1.50	2.84	138.8	0.1424	3.27	100%	4.11
33	1.911	1.49	1.63	139.6	0.2000	4.46	97%	5.52
34	2.000	1.49	2.55	136.4	0.1058	3.99	100%	3.66
35	1.918	1.47	1.52	138.9	0.0889	6.31	93%	3.94
36	1.999	1.49	2.32	135.4	0.0980	4.41	100%	3.63
37	1.699	1.44	1.77	139.9	0.1318	5.45	100%	3.92
38	1.970	1.50	1.80	140.0	0.0873	5.74	100%	3.58

Table S6. The measured versus predicted concentrations for each setpoint in the self-optimization experiments.

Entry	NMR Measured Concentration (M)				Predicted Concentration (M)			
	Triazole 1	Acrylonitrile 3	Product 4	Isomer 5	Triazole 1	Acrylonitrile 3	Product 4	Isomer 5
1 (LHC)	0.6933	1.3626	0.5829	0.0626	0.4972	1.2411	0.7756	0.0770
2 (LHC)	0.4739	1.2475	0.5482	0.0596	0.2909	1.2490	0.7097	0.0772
3 (LHC)	0.5706	0.7403	0.3553	0.0448	0.4782	0.6131	0.3490	0.0617
4 (LHC)	0.7437	0.9426	0.2033	0.0242	0.6744	0.9743	0.2579	0.0357
5 (LHC)	0.2376	0.8498	0.9065	0.1013	0.2563	0.8310	1.0299	0.1312
6 (LHC)	0.6706	0.5684	0.4442	0.0508	0.5754	0.6407	0.4524	0.0767
7 (LHC)	0.6807	0.5943	0.2646	0.0354	0.3637	0.8485	0.2659	0.0469
8 (LHC)	0.2420	1.0529	1.0351	0.1118	0.2481	1.1378	1.0846	0.1256
9 (LHC)	0.5469	0.7447	0.5814	0.0715	0.5358	0.8570	0.5640	0.0850
10 (LHC	0.0370	0.8481	0.6521	0.0740	0.0000	0.7515	0.6482	0.1336
11	0.1448	0.4241	1.0227	0.1117	0.1642	0.4562	1.0851	0.1943
12	0.0025	1.0941	1.1382	0.1091	0.0000	1.2123	1.4055	0.1950
13	0.0016	1.0929	1.3486	0.1217	0.0000	1.1961	1.4289	0.1886
14	0.0025	1.2253	1.3460	0.1253	0.0000	1.4288	1.4039	0.1646
15	0.0039	1.2646	1.2488	0.1201	0.0000	1.4715	1.4180	0.1664
16	0.0118	0.6414	1.3053	0.1284	0.0078	0.7570	1.2375	0.1878
17	0.0027	0.9115	1.3599	0.1294	0.0000	1.0225	1.3485	0.1759
18	0.0030	0.9826	1.3278	0.1300	0.0208	1.0654	1.3217	0.1686
19	0.0880	1.0361	1.2476	0.1281	0.1176	1.4731	1.2440	0.1352
20	0.2700	1.2184	1.0929	0.1158	0.2784	1.4419	1.0691	0.1146
21	0.0031	1.3697	1.3785	0.1136	0.0000	1.4305	1.3982	0.1739
22	0.0030	1.0062	1.1695	0.1151	0.0249	0.8620	1.3057	0.1825
23	0.0031	1.2831	1.4314	0.1349	0.0000	1.5095	1.3889	0.1522
24	0.0045	1.3811	1.3282	0.1284	0.0250	1.4580	1.3752	0.1474
25	0.2818	1.3289	1.2001	0.1249	0.2415	1.5810	1.1783	0.1186
26	0.0036	1.2120	1.3479	0.1286	0.0132	1.2904	1.3263	0.1559
27	0.0036	1.0610	1.4409	0.1176	0.0000	1.2032	1.4203	0.1879
28	0.0829	1.1146	1.2402	0.1241	0.0680	1.2550	1.2158	0.1452
29	0.0051	1.3001	1.3038	0.1278	0.0245	1.3635	1.3564	0.1516
30	0.0050	1.2614	1.3343	0.1310	0.0031	1.4188	1.3576	0.1527
31	0.0038	1.2443	1.2791	0.1022	0.0000	1.2477	1.5982	0.2369
32	0.0340	1.0638	1.0037	0.1047	0.0000	1.3132	1.4356	0.1827
33	0.0037	1.3199	1.3946	0.1148	0.0000	1.4267	1.4583	0.1820
34	0.1105	1.2149	1.3413	0.1343	0.0614	1.4516	1.3105	0.1420
35	0.0038	1.4268	1.3818	0.1194	0.0000	1.4850	1.4273	0.1650
36	0.0035	1.0601	1.3070	0.1270	0.0082	1.0637	1.3128	0.1692
37	0.0024	1.3310	1.4253	0.1319	0.0000	1.4934	1.3996	0.1549
38	0.0036	1.3877	1.3898	0.1306	0.0658	1.5392	1.3396	0.1413

12   Further *In Silico* Optimization

From the validated kinetic model, we also showed that the Matlab TSEMO script could be used for *in silico* optimization, allowing a large number of possibilities to be rapidly screened (**Figure S19**). To demonstrate and visualize this, 5000 random results were generated (green), followed by 200 sets of conditions chose by the TSEMO optimizer (red). The TSEMO algorithm clearly provides numerous sets of optimal conditions, compared with the randomly sampled background.
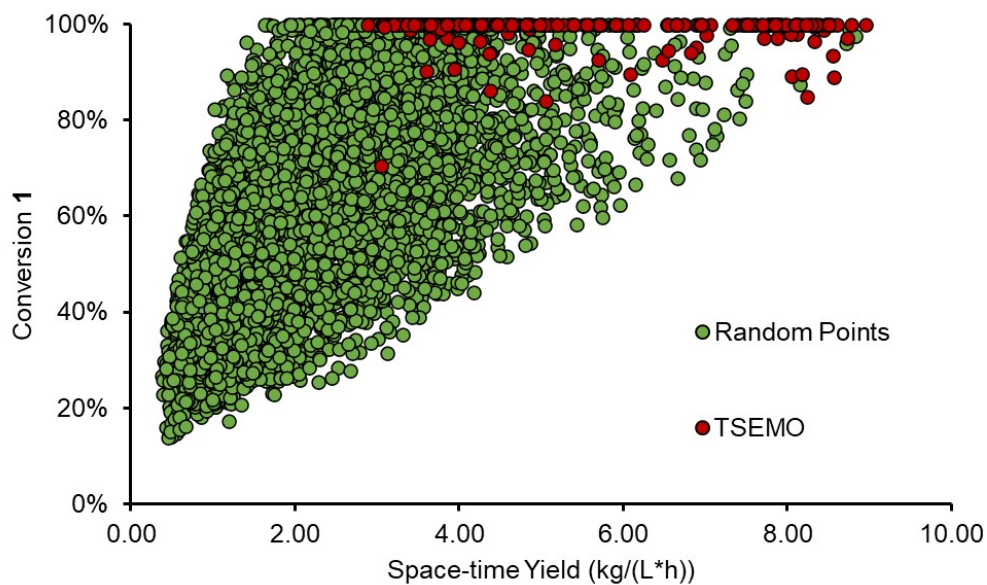
Figure S19. Graph of all results from *in silico* optimization using the multi-ramp kinetic model. The points in green are 5000 randomly selected combinations of conditions. Points in red are 200 conditions selected by the TSEMO algorithm (after an initial Latin hypercube of 10 conditions).

13   References

1   Data set available online at: https://doi.org/10.5281/zenodo.7829130

2   P. Sagmeister, F. F. Ort, C. E. Jusner, D. Hebrault, T. Tampone, F. G. Buono, J. D. Williams and C. O. Kappe, *Adv. Sci.*, 2022, **9**, 2105547.

3   A. M. Schweidtmann, A. D. Clayton, N. Holmes, E. Bradford, R. A. Bourne and A. A. Lapkin, *Chem. Eng. J.*, 2018, **352**, 277–282.